PERGAMON

International Journal of Heat and Mass Transfer 43 (2000) 2859–2868

International Journal of HEAT and MASS TRANSFER

www.elsevier.com/locate/ijhmt

Laminar film condensation along a vertical fin

F. Méndez[a], J.J. Lizardi[b], C. Treviño[b,*]

[a]Facultad de Ingeniería, UNAM, 04510 México D.F., Mexico
[b]Facultad de Ciencias, UNAM, 04510 México D.F., Mexico

Received 3 May 1999; received in revised form 1 November 1999

Abstract

We study the conjugate condensation-heat conduction process of a saturated vapor in contact with a vertical fin, including both longitudinal and transversal heat conduction effects. The momentum and energy balance equations are reduced to a nonlinear system of partial differential equations with four parameters: the Prandtl number, Pr_c, Jakob number, Ja, a nondimensional fin thermal conductivity α and the aspect ratio of the plate ε. Using the small Jakob limit and the boundary layer approximation, the total mass flow rate of condensed fluid has been obtained for all possible values of the involved parametric space. © 2000 Elsevier Science Ltd. All rights reserved.

Keywords: Film condensation; Conjugate heat transfer

1. Introduction

The heat transfer analysis of film condensation is an important area in the design of heat exchangers. Here, we are interested in studying the laminar film condensation over fins, where fundamental and practical physical aspects of the problem have a clear influence on the design and control of fin performance. Since the pioneering paper of Nusselt [1], simplifications and idealizations have been re-examined during the past decades in order to improve the simple Nusselt's theory. One of these situations that serve to define more realistic models and to select properly the heat-transfer characteristics, appears when the conjugate heat transfer problem is taken into account. From this point of view, we accept that the conjugate problem is described by the thermal interaction between the fin and the adjacent laminar boundary layer film of the condensate. It is then necessary to consider non-isothermal conditions in the fin in order to have an adequate description of the involved phenomena. Well-recognized works mostly deal with film condensation over isothermal walls. Sparrow and Gregg [2], among others, solved numerically a set of partial differential governing equations for the gravity driven laminar film condensation on a vertical flat plate. They employed boundary layer theory and similarity methods for a plate at uniform temperature. They showed that the influence of the inertial terms are not important, if the Prandtl number is larger than 10, and were quite small even for a Prandtl number of order unity. The importance of such results has been well known and documented in Ref. [3], extended by Koh et al. [4], Koh [5] and Chen [6]. In general, the state-of-the-art with isothermal surfaces can be found in Ref. [7] and more recently, in [8].

Although the foregoing works are essential contributions to the study of laminar film condensation, they were only reserved for those situations where the temperature at the surface of the plate has been maintained uniformly. We notice here that this situ-

* Corresponding author.

0017-9310/00/$ - see front matter
PII: S0017-9310(99)00354-3

Nomenclature

c_c	specific heat of the condensed fluid
f_c	nondimensional stream function introduced in Eq. (19)
g	acceleration due to gravity
h	half-thickness of the fin
h_{fg}	latent heat of condensation
Ja	Jacob number defined in Eq. (2)
L	length of the fin
m'	mass flow rate of condensed fluid
Pr_c	Prandtl number of the condensed fluid
T	temperature
T_0	temperature at the base of the fin
T_s	temperature of the saturated vapor
$\bar{u}$, $\bar{v}$	longitudinal and transversal velocities in physical units
u, v	nondimensional longitudinal and transversal velocities
u_c	characteristic longitudinal velocity of the condensed fluid
x, y	Cartesian coordinates
z	nondimensional transversal coordinate of the plate defined in Eq. (14)

Greek symbols

α	heat conduction parameter defined in Eq. (10)
β	nondimensional parameter $\beta = \varepsilon^2/\alpha^{8/7}$
Δ	normalized thickness of the condensed layer
δ_c	thickness of the condensed layer
η	fin efficiency defined in Eq. (56)
ε	aspect ratio of the plate defined in Eq. (10)
η_c	nondimensional transversal coordinate for the condensed fluid flow
ϕ	nondimensional function introduced in Eq. (39)
λ_c	thermal conductivity of the condensed phase
λ_w	thermal conductivity of the fin
μ_c	dynamic viscosity of the condensed fluid
ν_c	kinematic coefficient of viscosity of the condensed fluid
ρ_c	condensed fluid density
θ_w	nondimensional temperature of the fin
θ_c	nondimensional temperature of the condensed layer
ξ	nondimensional inner coordinate defined in Eq. (45)
χ	nondimensional longitudinal coordinate defined in Eq. (14)
ζ	nondimensional inner coordinate defined in Eq. (39)

Subscripts

c	refers to the condensed fluid
f	conditions at the base of the fin
w	conditions at the fin

ation is only valid for very idealized cases. This was recognized by Patankar and Sparrow [9] in their numerical study of laminar film condensation on a vertical fin attached to a cooled vertical plate or cylinder. In this work, the condensation process is coupled with the heat conduction within the fin. They used a similarity analysis and concluded that the calculated fin heat transfer is lower than the predicted value obtained by using an isothermal fin model. Wilkins [10] has shown that an explicit analytical solution is possible for the formulation of Patankar and Sparrow. These contributions reveal that the studies of condensation on extended surfaces form a class by themselves and, for these problems, an estimation of surface area requirements for a condenser using the classical Nusselt analysis is not appropriate. Sarma and Chary [11] studied the condensation process on a vertical fin of variable thickness. By matching the governing equations of the vertical fin and the condensed phase, through appropriate wall condition, they have analyzed the effect of fin geometry on condensation heat transfer and, they found that the influence of this thermal interaction is of primordial importance. For practically, the same problem with uniform thickness of the fin, Chen et al. [12] solved the coupled interaction in the presence of the shear stress at the liquid–vapor interface, pointing out the influence of the dimensionless Prandtl number, Pr, Jacob number, Ja on the Nusselt number, Nu. Experimental results on film condensation have been correlated by Chen et al. [13]. Recently, Méndez and Treviño [14] solved the problem (using perturbation and numerical techniques) of laminar film condensation on a surface of a thin vertical plate caused by a forced cooling fluid. They showed that the effect of heat conduction through the plate modifies substantially the classical Nusselt solution. Similar results were reported in later works [15,16]. Film condensation transient effects were also considered by Flik and Tien [17], among others, where the transient film thickness is predicted using a simple method to study the propagation of the resulting traveling wave.

In order to obtain new solutions where non-isothermal conditions are present, in this paper we analyze the conjugate laminar film condensation on the external sides of a vertical fin. Here we consider the case for which the base of the fin is maintained at a uniform temperature. The heat flux from the condensed phase to the fin is strongly influenced by the presence of the extended surface with finite thermal conductivity because longitudinal and transverse heat conduction effects become significant. The coupling between the vertical fin and the condensed phase offers new theoretical perspective to the earlier fundamental works on laminar film condensation. In this work, we use perturbation methods and the boundary layer description for the condensed fluid flow to show that the longitudinal and transverse heat conduction through the plate depend on four nondimensional parameters: the Prandtl number, Pr_c, Jakob number, Ja, α and ε. Parameter α represents the ratio of the conductance (inverse of resistance) of longitudinal heat conduction in the fin to conductance for transverse heat convection through the condensate and ε is the aspect ratio of the fin. We develop an analysis for all values of α and in some cases, we compare the analytical solutions with the results obtained using numerical techniques.

2. Formulation and order of magnitude analysis

The physical model under study is shown in Fig. 1. A thin vertical fin, with length L and thickness $2h$ with $2h \ll L$, is immersed in a stagnant atmosphere filled with saturated vapor with a temperature T_s. The fin's base is maintained at a temperature $T_0 < T_s$, thus generating a heat flux from the saturated vapor and creating thin condensed films on both sides of the fin. We neglect the condensation effects over the top of the fin, due to the involved geometry scales. Also, for simplicity we consider that the top of the fin is adiabatic.

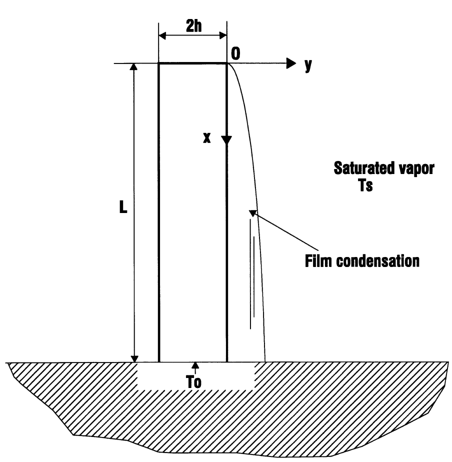

Fig. 1. Physical model sketch.

The inclusion of a finite thermal conductivity of the fin material, enables heat conduction in both longitudinal and transversal coordinates (x and y, respectively) through the extended surface. The condensate layers develop and drain with increasing thicknesses downstream. Due to the symmetry of the physical model, we only consider, for convenience, the right-hand side of this configuration. Therefore, we select the upper right corner of the fin as the origin of the coordinate system, whose y axis points in the direction normal to the vertical fin and its x axis points down in the longitudinal direction of the fin, that is, in the direction of the gravity vector. An order of magnitude estimate (see, for example, Ref. [18]) is useful to obtain the important nondimensional parameters and the relevant working regimes.

From the momentum equation for condensate flow in the longitudinal direction x, it can be shown that the condensed fluid's longitudinal velocity is of the order, $u_c \sim (g/\nu_c)\delta_c^2(x)$, where $\delta_c(x)$ is the condensed layer thickness, g is the gravity acceleration and ν_c is the kinematic coefficient of viscosity. The condensate mass flow and the condensation rates are of the order

$$m' \sim \frac{\rho_c g}{\nu_c}\delta_c^3(x), \quad \frac{\mathrm{d}m'}{\mathrm{d}x} \sim \frac{\lambda_c \Delta T_c}{\delta_c(x) h_{fg}},$$

respectively. The last relationship was obtained from the thermal energy balance at the condensate–vapor interface. Here, h_{fg} corresponds to the latent heat of condensation, λ_c represents the thermal conductivity of the condensed phase and ΔT_c is the characteristic temperature difference across the condensed liquid. Therefore, we show that a representative global thickness of the condensate layer related to the length of the fin is of order

$$\frac{\delta_{cf}}{L} \sim \left(\frac{Ja}{\gamma}\frac{\Delta T_c}{\Delta T}\right)^{1/4}, \quad \text{with } \gamma \equiv \frac{gL^3}{\nu_c^2}. \tag{1}$$

Ja corresponds to a suitable Jakob number that represents the ratio of the heat conducted through the liquid to the latent heat released during condensation, that is

$$Ja = \frac{C\lambda_c \Delta T}{\nu_c \rho_c h_{fg}}. \tag{2}$$

Here, $\Delta T = T_s - T_0$, Pr_c is the Prandtl number, $Pr_c = \nu_c \rho_c c_c/\lambda_c$ and c_c is the specific heat capacity. C is a numerical constant adopted to normalize the nondimensional condensate thickness to be shown later, $C = 4$. In general, the Jakob number is very small compared with unity [19] and thus, we can use the boundary layer approximation for the condensed fluid flow in the limit $Ja/\gamma \rightarrow 0$. The nondimensional velocity or Reynolds number for the condensed phase,

$Re_c = u_c L/\nu_c$, associated with the condensation process, is then of the order of $Re_c = O(Ja\,\gamma)^{1/2}$. Then, the condensed fluid velocity must be of order

$$u_c \sim \sqrt{\frac{gLJa\Delta T_c}{\Delta T}}. \tag{3}$$

On the other hand, from the physical model we have the same order of magnitude for the heat flux from the saturated vapor up to the fin base and this relationship is given by

$$\lambda_c L \frac{\Delta T_c}{\delta_{cf}} \sim \lambda_w h \frac{\Delta T_{wL}}{L}, \tag{4}$$

where λ_w represents the thermal conductivity of the fin and ΔT_{wL} is the characteristic longitudinal temperature difference along the fin. Also, the total temperature drop, ΔT, from the condensed fluid to the base of the fin is related to each part of the system as

$$\frac{\Delta T_c}{\Delta T} + \frac{\Delta T_{wL}}{\Delta T} \sim 1. \tag{5}$$

Finally, the heat flux balance at the vertical side of the fin is given by

$$\lambda_c \frac{\Delta T_c}{\delta_{cf}} \sim \lambda_w \frac{\Delta T_w}{h}, \tag{6}$$

where ΔT_w is the characteristic transverse temperature difference across the fin. Using the relationships (4)–(6) together with (1) for δ_{cf}, we obtain that the temperature drop at the condensed fluid, ΔT_c, is related to the total temperature drop, ΔT, as

$$\frac{\Delta T_c}{\Delta T} \sim \alpha^{4/3} \left(\frac{\Delta T_{wL}}{\Delta T} \right)^{4/3} \tag{7}$$

and equivalently

$$\frac{\Delta T_w}{\Delta T} \sim \varepsilon^2 \frac{\Delta T_{wL}}{\Delta T}. \tag{8}$$

Combining the order relationships (7) and (5), we obtain

$$\frac{\Delta T_{wL}}{\Delta T} + \alpha^{4/3} \left(\frac{\Delta T_{wL}}{\Delta T} \right)^{4/3} \sim 1, \tag{9}$$

where the parameters α and ε are defined by

$$\alpha = \frac{\lambda_w}{\lambda_c} \frac{h}{L} \left(\frac{Ja}{\gamma} \right)^{1/4} \quad \text{and} \quad \varepsilon = \frac{h}{L}. \tag{10}$$

The parameter α signifies the relative case of the heat conducted by the fin in the longitudinal direction as compared to the heat conducted through the condensate film. Thus, we can distinguish three relevant limits depending on the assumed values of α. For $\alpha \gg 1$, the heat conducted through the condensate film has most of the thermal resistance and longitudinal heat flow through the fin has negligible resistance. Thus, no temperature gradients of importance arise in the longitudinal direction. On the other hand, for $\alpha < 1$, resistance to heat flow through condensate film is much smaller than heat conduction in the fin in the longitudinal direction, producing large longitudinal temperature gradients on the plate. We assume that the aspect ratio of the plate, $\varepsilon = h/L$, always is very small compared with unity. Therefore, from the order relationships (7)–(9), we obtain

$$\frac{\Delta T_{wL}}{\Delta T} \sim \frac{1}{\alpha}, \quad \frac{\Delta T_w}{\Delta T} \sim \frac{\varepsilon^2}{\alpha}, \quad \frac{\Delta T_c}{\Delta T} \sim 1, \quad \text{for } \alpha \gg 1, \tag{11}$$

$$\frac{\Delta T_{wL}}{\Delta T} \sim 1, \quad \frac{\Delta T_w}{\Delta T} \sim \varepsilon^2, \quad \frac{\Delta T_c}{\Delta T} \sim 1, \quad \text{for } \alpha \sim 1 \tag{12}$$

and

$$\frac{\Delta T_{wL}}{\Delta T} \sim 1, \quad \frac{\Delta T_w}{\Delta T} \sim \varepsilon^2, \quad \frac{\Delta T_c}{\Delta T} \sim \alpha^{4/3}, \quad \text{for } \alpha \ll 1, \tag{13}$$

which clearly confirm the foregoing comments.

3. Governing equations

Introducing the following nondimensional variables

Solid

$$\theta_w(\chi, z) = \frac{T_s - T_w(x, y)}{T_s - T_0}; \quad \chi = \frac{x}{L}, z = \frac{y + h}{h}, \tag{14}$$

Condensed flow

$$\theta_c(\chi, \eta_c) = \frac{T_s - T_c(x, y)}{T_s - T_0}, \qquad \Delta(\chi) = \frac{\delta_c(x)}{L(Ja/\gamma)^{1/4}}, \eta_c = \frac{y}{\delta_c(x)}, \tag{15}$$

the heat conduction equation for the fin can be written as

$$\frac{\partial^2 \theta_w}{\partial \chi^2} + \frac{1}{\varepsilon^2} \frac{\partial^2 \theta_w}{\partial z^2} = 0. \tag{16}$$

Herein, the variables with the subscript c denote the variables of the condensed phase, those with w denote the variables of the fin. We supposed for simplicity that the top of the fin was adiabatic. Thus, the corresponding boundary conditions in the longitudinal direction at the tip ($\chi = 0$) and the base ($\chi = 1$) are given by

$$\left.\frac{\partial \theta_w}{\partial \chi}\right|_{\chi=0} = 0 \quad \text{and} \quad \theta_w(1, z) = 1 \tag{17}$$

and for the transversal direction

$$\left.\frac{\partial \theta_w}{\partial z}\right|_{z=0} = 0 \quad \text{and} \quad \left.\frac{\partial \theta_w}{\partial z}\right|_{z=1} = \frac{\varepsilon^2}{\alpha}\frac{1}{\Delta}\left.\frac{\partial \theta_c}{\partial \eta_c}\right|_{\eta_c=0}. \tag{18}$$

Introducing the nondimensional stream function f_c defined by

$$u = \frac{\bar{u}}{\sqrt{gLJa}} = \Delta^2 \frac{\partial f_c}{\partial \eta_c};\qquad v = \frac{\bar{v}\gamma^{1/4}}{Ja^{3/4}\sqrt{gL}} = -\frac{\partial(\Delta^3 f_c)}{\partial \chi} + \Delta^2 \eta_c \frac{d\Delta}{d\chi}\frac{\partial f_c}{\partial \eta_c}, \tag{19}$$

where $\bar{u}$ and $\bar{v}$ represent the longitudinal and transversal velocity components in physical units, respectively, the momentum and energy equations for the condensed liquid, using the boundary layer approximation, take the form

$$\frac{\partial^3 f_c}{\partial \eta_c^3} + 1 = Ja\Delta^4\left\{\frac{\partial f_c}{\partial \eta_c}\frac{\partial^2 f_c}{\partial \chi \partial \eta_c} - \frac{\partial f_c}{\partial \chi}\frac{\partial f_c}{\partial \eta_c} + \frac{1}{\Delta}\frac{d\Delta}{d\chi}\left[2\left(\frac{\partial f_c}{\partial \eta_c}\right)^2 - 3f_c\frac{\partial^2 f_c}{\partial \eta_c^2}\right]\right\} \tag{20}$$

$$\frac{\partial^2 \theta_c}{\partial \eta_c^2} = Ja\, Pr_c \Delta^4\left\{\frac{\partial f_c}{\partial \eta_c}\frac{\partial \theta_c}{\partial \chi} - \frac{\partial f_c}{\partial \chi}\frac{\partial \theta_c}{\partial \eta_c} - \frac{3}{\Delta}\frac{d\Delta}{d\chi}f_c\frac{\partial \theta_c}{\partial \eta_c}\right\}. \tag{21}$$

The boundary conditions associated with the condensed fluid governing equations are

$$\theta_c(\chi, 0) - \theta_w(\chi) = f_c(\chi, 0) = \frac{\partial f_c}{\partial \eta_c} = 0 \quad \text{at}\ \eta_c = 0 \tag{22}$$

$$\theta_c(\chi, 1) = \frac{\partial^2 f_c}{\partial \eta_c^2} = 0 \quad \text{at}\ \eta_c = 1. \tag{23}$$

The second condition of Eq. (23) arises from the balance of tangential shear stresses at the interface [7]. The normalized nondimensional thickness of the condensed film, Δ, is unknown and must be obtained from the analysis. The energy balance at the condensate–vapor interface gives the evolution of Δ as

$$4\Delta\frac{d[\Delta^3 f_c(\chi, 1)]}{d\chi} = -\left.\frac{\partial \theta_c}{\partial \eta_c}\right|_{\eta_c=1}, \tag{24}$$

with the initial condition $\Delta(\chi = 0) = 0$. The solution of the problem (16)–(24), should provide

$$\theta_w = \theta_w(\chi, z : \alpha, \varepsilon, Pr_c, Ja).$$

In the remainder of this paper, we classify the solutions according to the assumed values of α, taking advantage of the fact that, in general, Ja and ε^2 are very small compared with unity. Under small Ja and ε, the right-hand side of Eqs. (20) and (21) can be dropped, and the solution of the governing equations for the condensate liquid (20)–(24) yield

$$\theta_c = \theta(\chi, 1) \quad \text{and} \quad f_c(\eta_c) = \frac{1}{2}\eta_c^2\left(1 - \frac{\eta_c}{3}\right). \tag{25}$$

A suitable nondimensional heat flux q'' at the wall is given by the appropriate or reduced Nussett number for this problem N_c^*

$$N_c^* \equiv \frac{q''L}{\lambda_c(T_s - T_0)}\left(\frac{Ja}{\gamma}\right)^{1/4} = -\frac{1}{\Delta}\left.\frac{\partial \theta_c}{\partial \eta_c}\right|_{\eta_c=0} = \frac{\theta_w(\chi, 1)}{\Delta}. \tag{26}$$

Thus, the nondimensional energy balance equation (24) at the interface vapor–condensed fluid transforms to

$$\frac{d\Delta^4}{d\chi} = \theta_w(\chi, 1). \tag{27}$$

4. Thermally thin wall regime

The thermally thin wall regime corresponds to the case when $\alpha/\varepsilon^2 \gg 1$. In this regime the temperature variations in the transverse direction in the plate are very small compared with the global temperature difference as predicted by the second relationships in Eqs. (11) and (12). Therefore, in this regime the temperature of the plate is assumed to depend only in the longitudinal coordinate. The heat conduction equation for the fin can be integrated along the transverse coordinate and after applying the boundary conditions (18) together with the nondimensional condensed fluid temperature profile given by Eq. (25), we obtain

$$\alpha\frac{d^2\theta_w}{d\chi^2} = \frac{\theta_w}{\Delta}. \tag{28}$$

In the following subsections, we study the limiting cases of $\alpha \gg 1$ and $\alpha \ll 1$, for the thermally thin wall regime.

4.1. Analysis for the limit $\alpha \gg 1$

The system of equations (27) and (28) and the corresponding boundary conditions (17), can be solved through a regular perturbation technique, using the inverse of α as the small parameter of expansion. For very large values of the parameter α, the nondimensional temperature of the plate, θ_w, changes very little (of order of α^{-1}) in the longitudinal direction as shown in relationship (11). In order to obtain a solution in this limit, we assume that the nondimensional temperature of the plate as well as the nondimensional condensed layer thickness can be expanded in the form

$$\theta_w(\chi) = \theta_0(\chi) + \sum_{j=1}^{\infty} \alpha^{-j}\theta_j(\chi), \tag{29}$$

$$\Delta(\chi) = \Delta_0(\chi) + \sum_{j=1}^{\infty} \alpha^{-j}\Delta_j(\chi). \tag{30}$$

Introducing these relationships into Eqs. (27) and (28), we obtain after collecting terms of the same power of α, the following sets of equations

$$\frac{d^2\theta_0}{d\chi^2} = 0, \quad \frac{d\Delta_0^4}{d\chi} = \theta_0, \quad \text{for } \alpha^0 \tag{31}$$

$$\frac{d^2\theta_1}{d\chi^2} = \frac{\theta_0}{\Delta_0}, \quad \frac{4d\left(\Delta_0^3\Delta_1\right)}{d\chi} = \theta_1, \quad \text{for } \alpha^{-1} \tag{32}$$

$$\frac{d^2\theta_2}{d\chi^2} = \frac{\theta_0}{\Delta_0}\left(\frac{\theta_1}{\theta_0} - \frac{\Delta_1}{\Delta_0}\right), \qquad \frac{d\left(4\Delta_0^3\Delta_2 + 6\Delta_0^2\Delta_1^2\right)}{d\chi} = \theta_2, \quad \text{for } \alpha^{-2} \tag{33}$$

etc., with the following initial and boundary conditions

$$\Delta_i(0) = \theta_0(1) - 1 = \left.\frac{d\theta_i}{d\chi}\right|_{\chi=0} = 0, \quad \text{for all } i \tag{34}$$

and

$$\theta_i(1) = 0, \quad \text{for all } i > 0. \tag{35}$$

Integration of Eq. (31) with the corresponding initial and boundary conditions (34) gives $\theta_0 = 1$ and $\Delta_0 = \chi^{1/4}$. Introducing the solutions for θ_0 and Δ_0 into Eq. (32) and integrating twice for the energy equation and once for the condensed layer thickness equation, Δ_1, we obtain after applying the appropriate initial and boundary conditions

$$\theta_1 = \frac{16}{21}\left(\chi^{7/4} - 1\right), \quad \Delta_1 = \frac{4}{21}\left(\frac{4}{11}\chi^2 - \chi^{1/4}\right) \tag{36}$$

and in a similar way for the second-order terms

$$\theta_2 = \frac{128}{1617}\chi^{7/2} - \frac{64}{147}\chi^{7/4} + \frac{192}{539},$$

$$\Delta_2 = \frac{8}{231}\chi^{1/4} - \frac{64}{22{,}869}\chi^{15/4}.$$

Therefore, up to the second order, the condensed layer thickness is given by

$$\Delta = \chi^{1/4}\left[1 - \frac{4}{21\alpha}\left(1 - \frac{4}{11}\chi^{7/4}\right) + \frac{8}{231\alpha^2}\left(1 - \frac{8}{99}\chi^{7/2}\right)\right] + O(\alpha^{-3}), \tag{37}$$

and the nondimensional plate temperature is

$$\theta_w = 1 - \frac{16}{21\alpha}\left(1 - \chi^{7/4}\right) + \frac{192}{539\alpha^2}\left(1 - \frac{11}{9}\chi^{7/4} + \frac{2}{9}\chi^{7/2}\right) + O(\alpha^{-3}). \tag{38}$$

The leading term on the right-hand side of the above equations reduces to the classical Nusselt solution [1] for an isothermal plate.

In order to complete this subsection, we present the method used for the numerical integration of the governing equations. We transform the boundary value problem to an initial value problem by introducing the following nondimensional variables

$$\zeta = \frac{\chi}{\alpha^{4/7}}, \quad \phi = \frac{\Delta^4}{\alpha^{4/7}}. \tag{39}$$

The equations transform to the parameter-free form

$$\frac{d^2\theta_w}{d\zeta^2} = \frac{\theta_w}{\phi^{1/4}} \quad \text{and} \quad \frac{d\phi}{d\zeta} = \theta_w, \tag{40}$$

with the definition $\theta_w(0) = \theta_l$, the initial conditions are

$$\frac{d\theta_w}{d\zeta} = \theta_w - \theta_l = \phi = 0 \quad \text{at } \zeta = 0, \tag{41}$$

for any initial value of $\theta_l < 1$. The calculations are performed until $\theta_w(\zeta_f) = 1$ is reached. The value of $\zeta_f(\theta_l)$ dictates the appropriate value of α as $\alpha = 1/\zeta_f^{7/4}$. The asymptotic solution for values of $\zeta \to 0$, needed to start the numerical integration, takes the form

$$\theta_\mathrm{w} \sim \theta_1 + \frac{16}{21}\theta_1^{3/4}\zeta^{7/4} + \cdots, \quad \phi \sim \theta_1\zeta \quad \text{for}\ \zeta \to 0. \tag{42}$$

As the value of α decreases, θ_1 also decreases, reaching the value of $\theta_1 = 0$ for a critical value of α, α^*, to be obtained as follows. For this critical value of α, one can verify that the equations have the following closed form solutions

$$\theta_\mathrm{w} = \frac{8}{42^4}\zeta^7 \quad \text{and} \quad \phi = \frac{1}{42^4}\zeta^8, \quad \text{for}\ \alpha = \alpha^*. \tag{43}$$

Here $\zeta_\mathrm{f} = 42^{4/7}/8^{1/7}$ and thus, $\alpha^* = 1/\zeta_\mathrm{f}^{7/4} = 8^{1/4}/42 = 0.040\ldots$. Therefore, the nondimensional thickness of the condensed layer at the base of the fin gives

$$\Delta_\mathrm{f}^* = \left(\frac{42\alpha^*}{8^2}\right)^{1/7} = \frac{1}{8^{7/28}} \doteq 0.5946. \tag{44}$$

4.2. Analysis for the limit $\alpha < \alpha^*$

For smaller values of $\alpha, \alpha < \alpha^*$, a boundary layer develops close to the base of the fin. In order to study the condensation process for very small values of α, we introduce the following stretched variables

$$\xi = \frac{1-\chi}{\alpha^{4/7}}, \quad \phi = \frac{\Delta^4}{\alpha^{4/7}}, \tag{45}$$

transforming the governing equations to

$$\frac{\mathrm{d}^2\theta_\mathrm{w}}{\mathrm{d}\xi^2} = \frac{\theta_\mathrm{w}}{\phi^{1/4}} \quad \text{and} \quad \frac{\mathrm{d}\phi}{\mathrm{d}\xi} = -\theta_\mathrm{w}, \tag{46}$$

with the boundary conditions

$$\theta_\mathrm{w} = 1 \quad \text{at}\ \xi = 0 \tag{47}$$

$$\theta_\mathrm{w} \to 0 \quad \text{and} \quad \phi \to 0 \quad \text{for}\ \xi \to \infty. \tag{48}$$

Eq. (46) can be written in the phase-space variables as

$$\phi^{1/4}\left[\theta_\mathrm{w}\frac{\mathrm{d}^2\theta_\mathrm{w}}{\mathrm{d}\phi^2} + \left(\frac{\mathrm{d}\theta_\mathrm{w}}{\mathrm{d}\phi}\right)^2\right] = 1, \tag{49}$$

with the initial condition $\theta_\mathrm{w}(0) = 0$, which also guarantees the adiabatic condition. The solution can be obtained in closed form as $\theta_\mathrm{w} = 8\phi^{7/8}/\sqrt{42}$, or using the second part of Eq. (46), we also obtain

$$\phi = \left[\phi_\mathrm{f}^{1/8} - \frac{1}{\sqrt{42}}\xi\right]^8 \quad \text{and} \quad \theta_\mathrm{w} = \frac{8}{\sqrt{42}}\left[\phi_\mathrm{f}^{1/8} - \frac{1}{\sqrt{42}}\xi\right]^7. \tag{50}$$

Here ϕ_f is the nondimensional value at the base of the fin and is given by $\phi_\mathrm{f} = (\sqrt{42}/8)^{8/7} \doteq 0.78608$. The nondimensional thickness of the condensed layer is then $\Delta_\mathrm{f} = \alpha^{1/7}\phi_\mathrm{f}^{1/4}$, for values of $\alpha \le \alpha^*$. For this case, the condensation layer begins at a very well defined position of the fin, $\xi_\mathrm{wet} = \sqrt{42}\phi_\mathrm{f}^{1/8} \doteq 6.2887$. At $\xi > \xi_\mathrm{wet}$ ($\chi_\mathrm{wet} = 1 - \xi_\mathrm{wet}\alpha^{4/7}$) there is no condensed fluid at all. The portion of the fin in contact with condensed fluid decreases as the value of α decreases. The fin wets completely for values of $\alpha \ge \alpha^*$.

5. Thermally thick wall regime

For values of α of the order of $\varepsilon^{7/4}$, the variations in the temperature in the transverse direction of the plate are now important and must be retained. Introducing the same inner variables given by (45), we obtain the following transformed governing equations

$$\beta\frac{\partial^2\theta_\mathrm{w}}{\partial\xi^2} + \frac{\partial^2\theta_\mathrm{w}}{\partial z^2} = 0 \tag{51}$$

$$\frac{\mathrm{d}\phi}{\mathrm{d}\xi} = -\theta_\mathrm{w} \tag{52}$$

where $\beta = \varepsilon^2/\alpha^{8/7}$. The boundary and initial conditions are then given by

$$\left.\frac{\partial\theta_\mathrm{w}}{\partial z}\right|_{z=1} = -\beta\frac{\theta_\mathrm{w}}{\phi^{1/4}}, \quad \left.\frac{\partial\theta_\mathrm{w}}{\partial z}\right|_{z=0} = 0 \tag{53}$$

$$\theta_\mathrm{w}(\xi = 0, z) - 1 = \left.\frac{\partial\theta_\mathrm{w}}{\partial\xi}\right|_{\xi\to\infty} = 0. \tag{54}$$

With the asymptotic limit of $\beta \to 0$, we recover the solution obtained in the previous subsection. The system of equations (51)–(54), were integrated numerically using a central finite-difference scheme for the Laplace

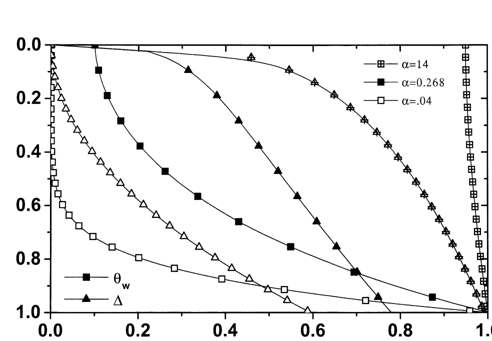

Fig. 2. Nondimensional temperature, θ_w (■) and thickness of the condensed film, Δ (▲) as a function of the nondimensional longitudinal coordinate χ, for different values of the parameter α in the thermally thin wall regime.

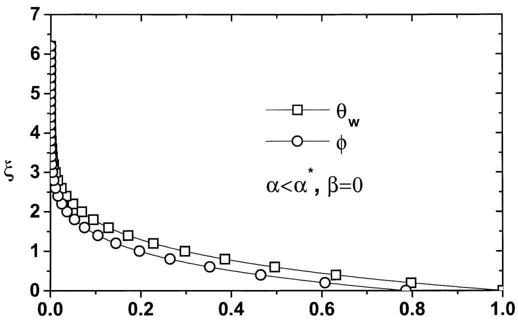

Fig. 3. Nondimensional temperature, θ_w (□) and modified thickness of the condensed film, ϕ (○) as a function of the nondimensional inner coordinate ξ, for $\alpha < \alpha^*$ in the thermally thin wall regime ($\beta = 0$).

equation and a conventional Simpson rule for Eq. (52). The iteration procedure is to assume a known initial distribution for the temperature θ_w, using a pseudo-temporal version of the Laplace equation. The steady-state solution is reached when a convergence criterion is fulfilled.

6. Results and conclusions

The analytical and numerical results are presented in this section through Figs. 2–7. Fig. 2 shows the numerical solution for the nondimensional temperature and condensed film thickness for different values of α in the thermally thin wall regime. For large values of α, the solution tends to the well-known Nusselt solution, with $\theta_w \sim 1$ and $\Delta \sim \chi^{1/4}$. As the value of α decreases, the temperature variations along the longitudinal coordinate are larger and the condensed mass flow decreases. There is a critical value of α, $\alpha^* = 0.0400\ldots$, which makes the temperature at the top of the fin to be exactly the same as the temperature of the saturated vapor, $\theta_w(\chi = 0) = 0$. The corresponding limiting analytical profiles for values of $\alpha \leq \alpha^*$ and $\beta = 0$ are plotted in Fig. 3. For values of $\alpha \leq \alpha^*$ and finite values of β, the nondimensional condensed layer film thickness Δ as a function of ξ is plotted in Fig. 4. The numerical results show that for even values of β of order unity, there is an important mass flow rate of condensed fluid. The portion of the fin in contact with the condensed fluid decreases with increasing values of β. In physical units, the mass flow rate of condensed fluid at the bottom of the fin is then given by

$$m' = \frac{\rho_c \nu_c^{1/2}}{3}\left[\frac{4g^{1/3}L\lambda_c(T_s - T_0)}{h_{fg}\mu_c}\right]^{3/4} \Delta_f^3(\alpha, \beta) \tag{55}$$

where the numerical solution for Δ_f is plotted in Figs. 5 and 6, for the thermally thin and thick wall approximations, respectively. In Fig. 5, the two-term asympto-

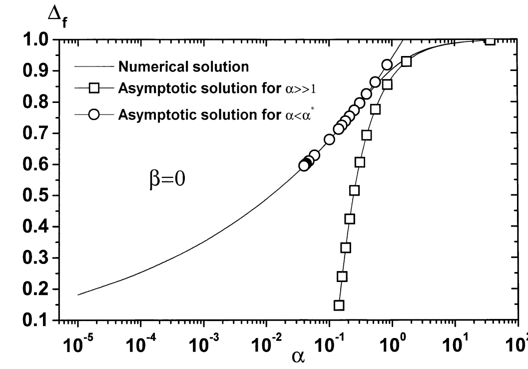

Fig. 5. Nondimensional thickness of the condensed film at the base of the fin, Δ_f as a function of α. The asymptotic solutions for $\alpha \gg 1$ (□) and $\alpha < \alpha^*$ (○) are also plotted.

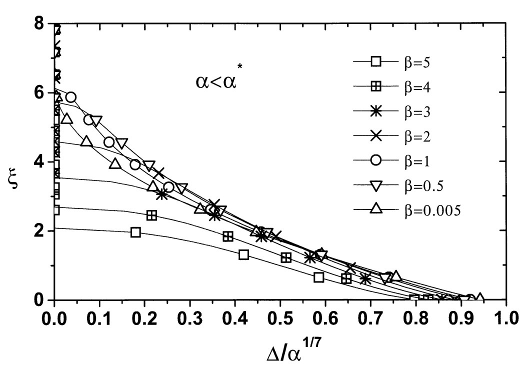

Fig. 4. Nondimensional reduced thickness of the condensed film, $\Delta/\alpha^{1/7}$ as a function of the nondimensional inner coordinate ξ, for different values of β in the thermally thick wall regime.

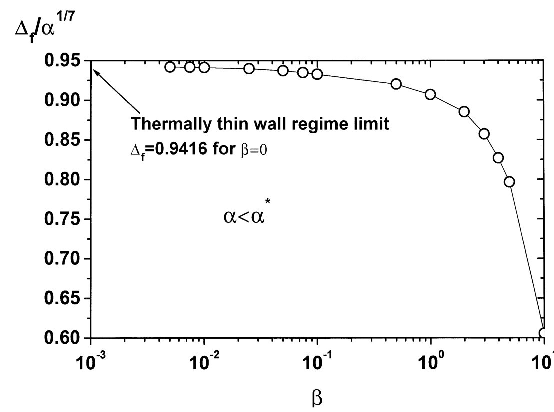

Fig. 6. Nondimensional reduced thickness of the condensed film at the base of the fin, $\Delta_f/\alpha^{1/7}$ as a function of β in the thermally thick wall regime.

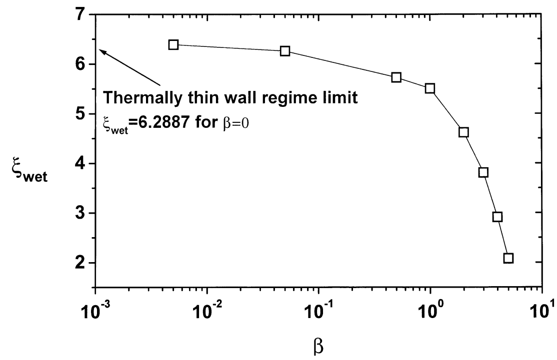

Fig. 7. Nondimensional wetted length, ξ_{wet}, as a function of β.

tic solutions for $\alpha \gg 1$ and the closed form solution for $\alpha \leq \alpha^*$ are also included. The solution for $\alpha \gg 1$, gives acceptable results for values of $\alpha \sim 2$, while the other approximation offers good results for values of $\alpha \sim 0.3$. Fig. 6 shows $\Delta_f/\alpha^{1/7}$ as a function of parameter β, for values of $\alpha \leq \alpha^*$. The effect of the finite aspect ratio of the fin, included in the definition of β, for a given value of α, is to reduce the value of Δ_f. If we define the fin efficiency as the ratio of the actual condensate mass flow rate to that obtained by using the isothermal wall ($\alpha \to \infty$), then

$$\eta = \frac{m'}{(m')_\infty} = \Delta_f^3, \tag{56}$$

with Δ_f obtained in Figs. 5 and 6 (for the thermally thin and thick wall regimes, respectively). In Fig. 5, we can see that the asymptotic solution obtained for the case of $\alpha < \alpha^*$ gives excellent results even for values of $\alpha < 0.3$, $\Delta_f = (0.9416 - 0.09\beta)\alpha^{1/7}$. Therefore, the efficiency can be written as

$$\eta \simeq (0.9416 - 0.09\beta)^3 \alpha^{3/7} \quad \text{for } \alpha < 0.3. \tag{57}$$

As illustration we computed typical nondimensional values of the important parameters by using a simple fin made of aluminum with dimensions $h = 0.5$ cm. and $L = 10$ cm. Three different condensed liquids have been used: R-113, water and NH_3. The adopted value of the temperature difference is $\Delta T = 20$ K. Table 1 summarizes the numerical results obtained for the parameters Ja, γ, α, β and η. The resulting Jakob numbers for the first two liquids are very low compared with unity and the results obtained in this work can be used. However, the results obtained with NH_3 are to be used with caution, because the convective terms in the governing equations now are important and must be included in the calculations. The obtained value of γ is always very small compared with unity. The value of α is of order unity for the first case, while for the other two liquids it is extremely low, even below α^*, indicating that in these cases, there is a portion of the plate which remains dry. In all three cases, we can assume that the thermally thin wall regime ($\beta \to 0$) represents a good approximation. Finally, the fin efficiency has been obtained using Eq. (57), which is an excellent approximation for values of $\alpha < 0.3$ and $\beta < 0.2$. Using R-113 for this fin configuration we obtain an efficiency of 35.8%, while the other two cases give an efficiency around 15%.

Table 1
Typical values of parameters obtained using different liquids of interest (the fin material, dimensions and operating conditions are explained in the text)

Liquid	Ja	γ	α	β	η
R-113	0.059	4.97×10^{10}	0.141	0.0235	0.358
H_2O	0.0223	1.23×10^{10}	0.02	0.218	0.147
NH_3	0.237	1.94×10^{11}	0.0234	0.183	0.158

In this paper, we studied the conjugate heat transfer condensation process of saturated vapor in a vertical fin with an uniform temperature at the bottom. This boundary condition modifies the results obtained in previous works, where the effect of the longitudinal heat conduction through the fin has been neglected in the thermally thick wall regime. In this particular case, the longitudinal heat conduction must be retained for any value of the parameter α. Furthermore, there is a critical value of α, $\alpha^* \doteq 0.0400\ldots$, where the temperature at the top of the fin reaches the temperature of the condensed vapor. For values of $\alpha < \alpha^*$, there is a portion of the fin which remains dry. Finally, Fig. 7 shows the nondimensional wetted length, ξ_{wet}, as a function of β. The total mass flow rate of condensed fluid has been obtained for all values of the involved parametric space.

Acknowledgements

This work has been supported by the grant 3658PA of CONACyT, Mexico.

References

[1] W. Nusselt, Z., Die oberflächenkondensation des wasserdampfes, Z. Ver. Dt. Ing. 60 (1916) 569–575, 541–546.
[2] E.M. Sparrow, J.L. Gregg, A boundary layer treatment of laminar-film condensation, Trans. Am. Soc. Mech. Engrs 81 (1959) 13–17.
[3] H. Merte Jr, Condensation heat transfer, Adv. Heat Transfer 15 (1973) 181–272.

[4] J.C.Y. Koh, E.M. Sparrow, J.P. Hartnett, The two phase boundary layer in laminar film condensation, Int. J. Heat Mass Transfer 2 (1961) 69–82.
[5] J.C.Y. Koh, On integral treatment of two-phase boundary layer in film condensation, J. Heat Transfer 83 (1961) 359–362.
[6] M.M. Chen, An analytical study of laminar film condensation. Part 1: flat plates, J. Heat Transfer 83 (1961) 48–54.
[7] J.W. Rose, Fundamentals of condensation heat transfer: laminar film condensation, JSME Int. J., Ser. 2 31 (1988) 357–375.
[8] I. Tanasawa, Advances in condensation heat transfer, Adv. Heat Transfer 21 (1991) 55–139.
[9] S.V. Patankar, E.M. Sparrow, Condensation on an extended surface, J. Heat Transfer 101 (1979) 434–440.
[10] J.E. Wilkins, Condensation on an extended surface, J. Heat Transfer 102 (1980) 186–187.
[11] P.K. Sarma, S.P. Chary, V. Dharma Rao, Condensation on a vertical plate fin of variable thickness, Int. J. Heat Mass Transfer 31 (1988) 1941–1944.
[12] H.T. Chen, Z. Lan, T.I. Wang, Study of conjugate conduction–laminar film condensation for a vertical plate fin, Int. J. Heat Mass Transfer 37 (1994) 2592–2597.
[13] S.L. Chen, M.F. Gerner, C.L. Tien, General film condensation correlations, Experimental Heat Transfer 1 (1987) 93–107.
[14] F. Méndez, C. Treviño, Film condensation generated by a forced cooling fluid, Eur. J. Mech. B/Fluids 15 (2) (1996) 217–240.
[15] C. Treviño, G. Becerra, F. Méndez, Laminar film condensation on a thin finite thickness plate, AIAA Journal of Thermophysics and Heat Transfer 11 (1997) 119–121.
[16] F. Méndez, C. Treviño, Film condensation induced by a natural convective flow: steady-state analysis, Int. J. Heat Mass Transfer 40 (1997) 1279–1289.
[17] M.I. Flik, L.C. Tien, An approximate analysis for general film condensation transients, J. Heat Transfer 111 (1989) 511–517.
[18] A. Bejan, Convection Heat Transfer, in: Wiley, New York, 1984, pp. 146–150.
[19] F.P. Incropera, D.P. De Witt, Fundamentals of Heat and Mass Transfer, Wiley, New York, 1996.